Journal of Ovonic Research Vol. 19, No. 2, March - April 2023, p. 219 - 230

Novel controlling pathway for metallic nanoparticles by laser assisted ion-reduction process

R. A. Shlaga, A. M. Alwan*, M. S. Mohammed
Department of Applied Science, University of Technology, Baghdad, Iraq

In this work, the morphological and plasmonic features of the AgNPs which formed by ion-reduction process was carried out extensively. The application of the laser beam during the ion- reduction process has significant effect in the reconstruction of the formed AgNPs with small dimensions and non-frequent morphologies, according to the laser illumination intensity. For non-illumination process the deposited form of the AgNPs appear aggregated into cluster of layer AgNPs size due to the chemical reaction at Si interface, the AgNPs sizes varied from 0.85 to1.2 μm; while at lower laser intensity of about 250 mW/cm^2 the AgNPs sizes varied from 0.1 to 1.0 μm, while at high intensity upto 400 mW/cm^2 the AgNPs sizes varied from 0.05 to 0.4 μm. The hot spot dimension for non-illumination process varied from 1 to 11 nm while at low intensity of 250 mW/cm^2 the hot spot dimension varied from 1to 8 nm. At high intensity upto 400 mW/cm^2, the hot spot varied from 0.1 to 14 nm. The XRD for the generated Ag nanoparticles / Si nanocrystallites, for non- illumination the grain size about 6.171 nm and SSD about 92.687 m^2/g while at low intensity of 250 mW/cm^2 the grain size about 4.759nm and SSD about 120.191 m^2/g. At high intensity of 350 mW/cm^2, the grain size about 2.037nm and SSD about 280.847m^2/g uniform distributed AgNPs with minimum hot spot regions can be realized with 350mW/cm^2 laser illumination intensity. This process is considerable as a novel work which can be adopted modification at the plasmonic features of metallic nanoparticles for SERs application.

(Received December 7, 2022; Accepted April 5, 2023)

Keywords: Metallic nanoparticles, Ion-reduction process, Pre-etching, Macro-porous

1. Introduction

Many potential applications of SERs sensors fabricated with ion-reduction process are highly dependent on the precise control of morphology for the plasmonic nanoparticles. However, the effects of key etching parameters, such as the concentration of metallic solution, and dipping time, on the morphology, metallic nanoparticles and hotspot regions have not been fully explored[1-3]. Over the past decades, there has been an enormous interest in nanostructure of nanoparticles and a lot of progress has been reported. In ion-reduction process, one-dimensional nanoparticles nanostructures, such as nanowires and Nano pillars, have been prepared for a wide range of applications, such as photovoltaics, nanoparticles chemical sensors and nanophotonic SERs sensors[4-7]. The procedure utilizes ion reduction process, where metallic nano structures are deposited on an etched silicon and porous silicon surface to catalyze the formation process[8-12]. The formation of plasmonic nanoparticles by ion-reduction process at room temperature was depended on the density of the ion reduction cluster, concentration of the metallic electrolyte with dipping time of the base substrate(etched Si layer) in the solution of the electrolyte[13]. As the concentration and the dipping time was increased the morphology of the deposited layer was modified towards increasing the metallic nano particles sizes and the surface tends to fully covered with high density of large size metallic nanoparticles. In this current work, a novel path way was suggested to modify the plasmonics and the morphological of AgNPs via employing the heating effects by the laser beam on the ion reduction process at different laser intensities. Extensive analysis was carried out to optimize the fabrication conditions.

* Corresponding author: alkrzsm@yahoo.com
https://doi.org/10.15251/JOR.2023.192.219

2. Procedure

A Si substrate (n-type) with an orientation of (100) and a resistivity of 10 Ω.cm was employed. The substrate was sliced into 1x1 cm^2 pieces, cleaned with 10% hydrofluoric acid in an ultrasonic path cleaner for 5 minutes. The creation of AgNPs was carried out using two separated process, the first one involve the normal pre etching of Si substrate. The substrate were placed in HF acid solution of 15% M concentration for a period 120 min time at room temperature under normal day light illumination. This process was performed for the purpose of increasing the density of dangling bonds (Si-H_x x=1,2,3,..) within the crystalline silicon surface and thus increasing the silver ion reduction centers for the creation of silver nanoparticles. This process results in a layer of AgNPs deposited naturally on the surface as a result of the reduction of silver ions by means of dangling bond the of crystalline silicon surface. As for the second process, which was a local heating process for both the surface of crystalline silver and AgNPs, and this was done by different laser beam intensities 250, 300,350, 400 mW/cm^2 with a wavelength of 405nm for a period 30 min, this process was done by dipping the crystalline Si substrates in silver nitrate solution of $AgNO_3$ of concentration $5*10^{-3}$M. The structural features were tested through using SEM and X-ray diffraction. Where the Image software program was employed to investigate the Ag nanoparticle size and hotspot histogram from SEM image.

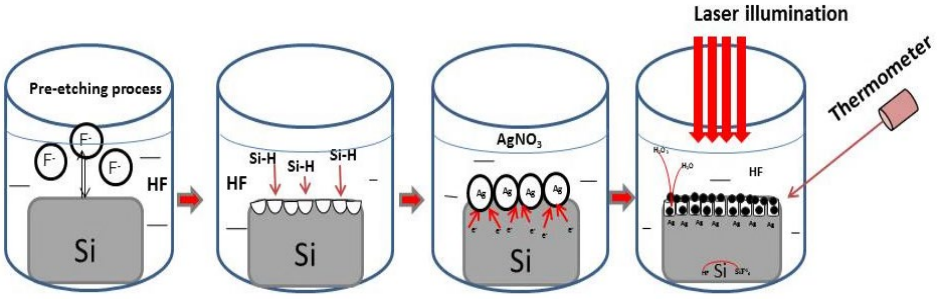

Fig. 1. Schematic view of the fabrication of Si nanostructures using ion reduction process.

As shown in figure 1, the laser thermometer was used to measure the local temperature during the irradiation process. The rising of the temperature will enhance the probability of the reconstruction surface morphologies of the crystalline silicon and the deposited AgNPs. The dependence of surface temperature on the laser power intensity is shown in figure 2. From this figure temperature is increased from 44C° at 250mW/cm^2 laser power density to 65.6C° at 400 mW/cm^2 laser power density. The temperture of the substrate was measured by repeating each condition eight times.

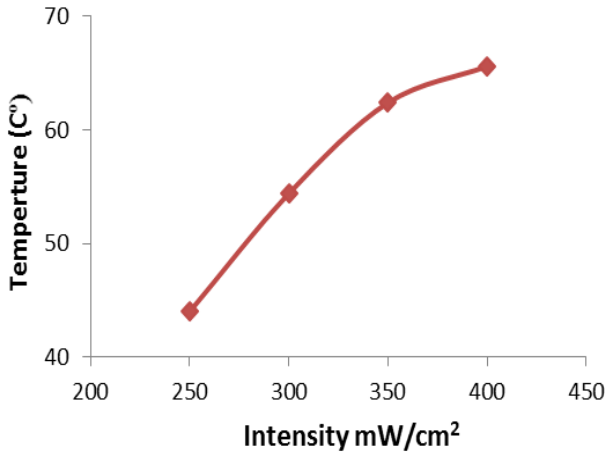

Fig. 2. Illustrates the relationship between intensity and temperature.

3. Results and discussion

3.1. Morphological features of Ag NPs

The FE-SEM image of surface morphology of the deposited AgNPs upon the surface of pre-etched crystalline silicon is shown in fig 3. From this figure it can be seen that the AgNPs looks-like aggregated non-connected nanoparticles due to natural Ag^{+1} reduction process by the dangling bonds of pre-etched surface.

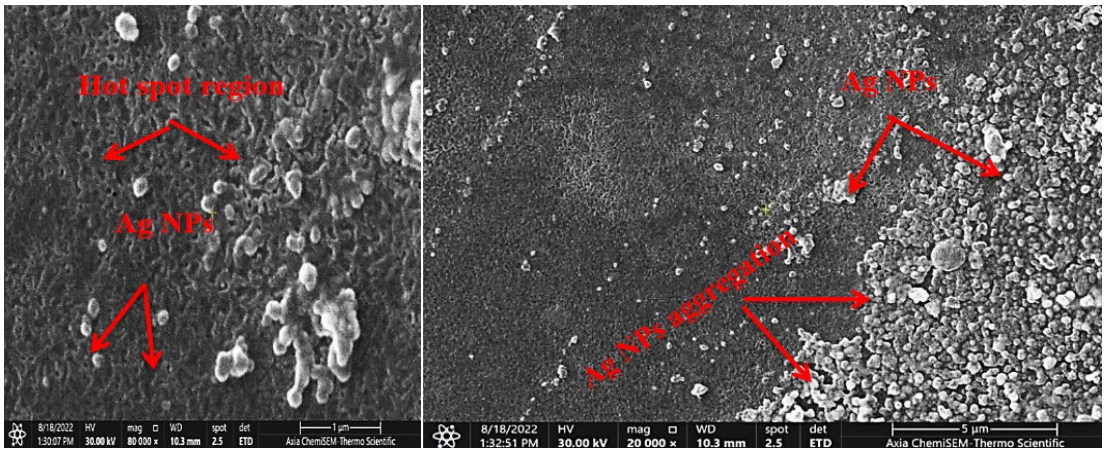

Fig. 3. Illustrates FE-SEM for Si immersed at 10^{-3} M $AgNO_3$ concentration and 30min reduction min.

When laser beams at different intensities are shined on the sample, the surface properties will change significantly due to the heating substrate through chemical reaction at Si interface, which leads to the emergence of various morphologies, due to various reconstruction behaviors as shown in FE-SEM of figures (4-7).

The first effect is concerned with low laser intensities of 250 mW/cm^2, where its radiation of laser, will results in heating the surface and thus improving the density of dangling bonds as shown in fig (4). When the intensity increases, these bonds increase, and therefore the nano size of AgNPs will decrease.

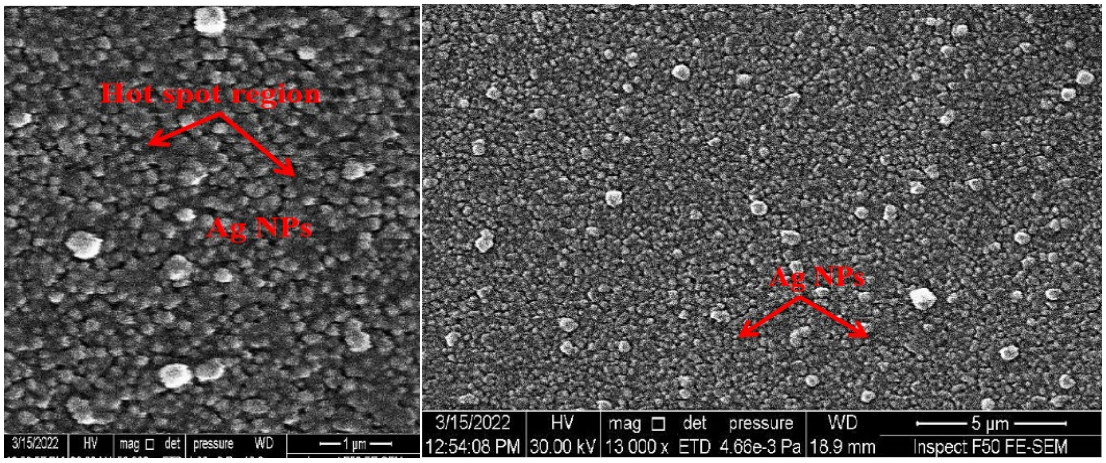

Fig. 4. Illustrates FE-SEM for Si immersed at $5*10^{-3}$ M $AgNO_3$ concentration and reduction time 30min with laser illumination 250 mW/cm^2.

It becomes clear to us that when the laser intensity is increased to 300 mW/cm^2, a new type of space distribution of silver nanoparticles will appeared as shown in fig(5). We have two distinct regions of relatively large nanoparticles separated by a region of small size silver nanoparticles. The emergence of this spatial distribution may be a result of the irregular distribution of the nucleation centers represented by the dangling bonds(Si-H), which increase intensity with the increase in the temperature of Si substrate. Also, the Gaussian distribution of the laser intensity plays an important role in the irregular spatial distribution of the ion-reduction centers (nucleation sites).

When the intensity increase up to 300 mW/cm^2, we notice that the formed layer was appeared consisted of the fine NPs structure with regular shape (nearly circular form) and inhomogeneous AgNPs particles was formed as shown in Fig 5.

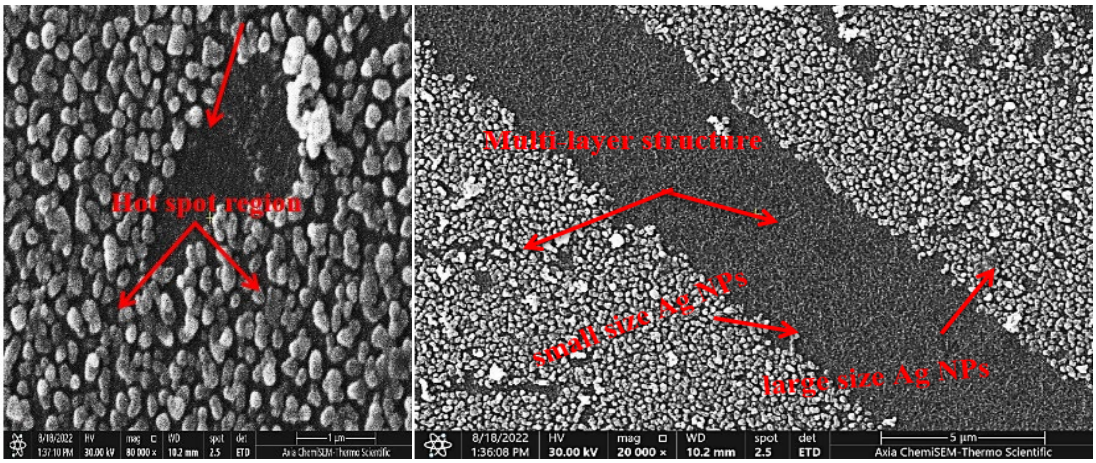

*Fig. 5. Illustrates FE-SEM for Si immersed at 5*10^{-3} M $AgNO_3$ concentration and reduction time 30 min with laser illumination 300 mW/cm^2.*

When the intensity become 350 mW/cm^2, the surface will completely coated with AgNPs which result on increase the dangling bonds and this will lead to haunt more of Ag NPs on the substrate as illustrated by fig 6. When the intensity of the laser beam is increased to 350 mW/cm^2 fig (6), it becomes clear to us the formation of homogenous and uniformly spaced layer of silver nanoparticles. This structure indicates the uniform distribution of nucleation sites which resulted from the uniform heat distribution along the silicon substrate, due to the role of HF acid in heating the Si substrate regularly.

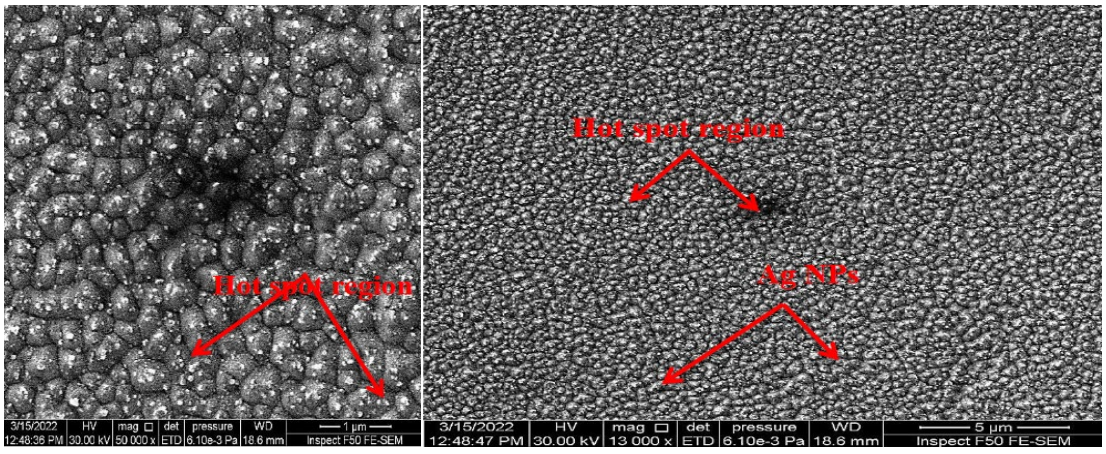

*Fig. 6. Illustrates FE-SEM for Si immersed at 5*10^{-3} M $AgNO_3$ concentration and reduction time 30 min with laser illumination 350 mW/cm^2.*

As shown in fig 7, with increasing the power density up to 400 mW/. The etching will increase in the base Si substrate and hence a macroporous Si layer will exist and the AgNPs will aggregated over pores boundaries. This type of structure was synthesized on the Si surface using a laser power density of about 400 mW/cm^2.

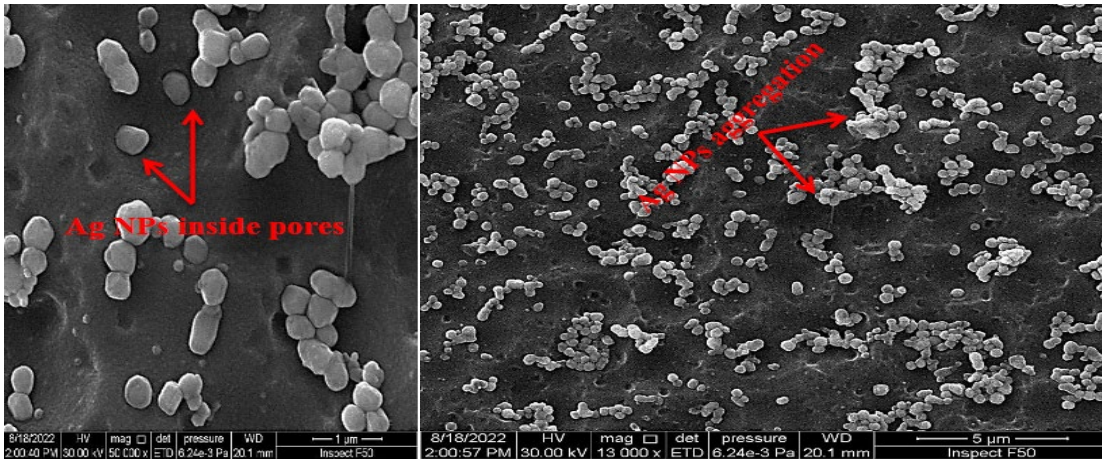

*Fig. 7. Illustrates FE-SEM for Si at 5*10^{-3} M $AgNO_3$ concentration and reduction time 30min with laser illumination 400 mW/cm^2.*

During the laser irradiation process, the rate of generation (e-h$^+$) pairs was increased with increasing the laser intensity due to the increasing of the substrate temperature (ΔT). The temperature (ΔT) is given by the following equation1:

$$\Delta T = P_h / m\, c_v \quad (1)$$

where P_h is the input heating power and its related with the internal equation efficiency of silicon η_{in} by the following equation 2. If the incident power increases the temperature will increase also P:

$$P_h = (1 - \eta_{in}) * P(1 - R_{substrate}) \quad (2)$$

Based on equation (2), $R_{substrate}$ represent the surface reflectivity of the substrate (with or without) the AgNPs. The integration of metallic nanoparticles on the Si surface process may increase the surface reflectivity but it will also improve the absorption of the incident photons due to the plasmonic effect of AgNPs sizes and effective role of hot spot regions. As the dimension of the AgNPs and hotspot vacancies decreases the localized surface plasmons was improved and these will acts as local antenna, so the laser – assisted silicon dissolution and laser assisted the redistribution process of AgNPs were improved. Controlling the laser intensity can be thought as a finger print of the surface feature (morphology of silicon and AgNPs). So, at higher illumination intensities the Si surface was converted from bulk to porous structure due to the light and heat generation (e-h$^+$) couples within the upper Si surface.

Based on the histogram depicted in figure (8), the sizes of AgNPs were varied from (0.85-1.2) µm for non-illumination substrate, while for the case of the illumination, the size of AgNPs was decreased with increasing the illumination intensity. The minimum AgNPs about (0.05-0.4) µm is achieved with 350mW/cm^2.

Also, the histogram of the hotspot vacancies among the AgNPs is shown in figure (9) for non-illumination substrate the dimension of hotspot vacancies is ranging from 1to 11 nm as the illumination intensity increased.

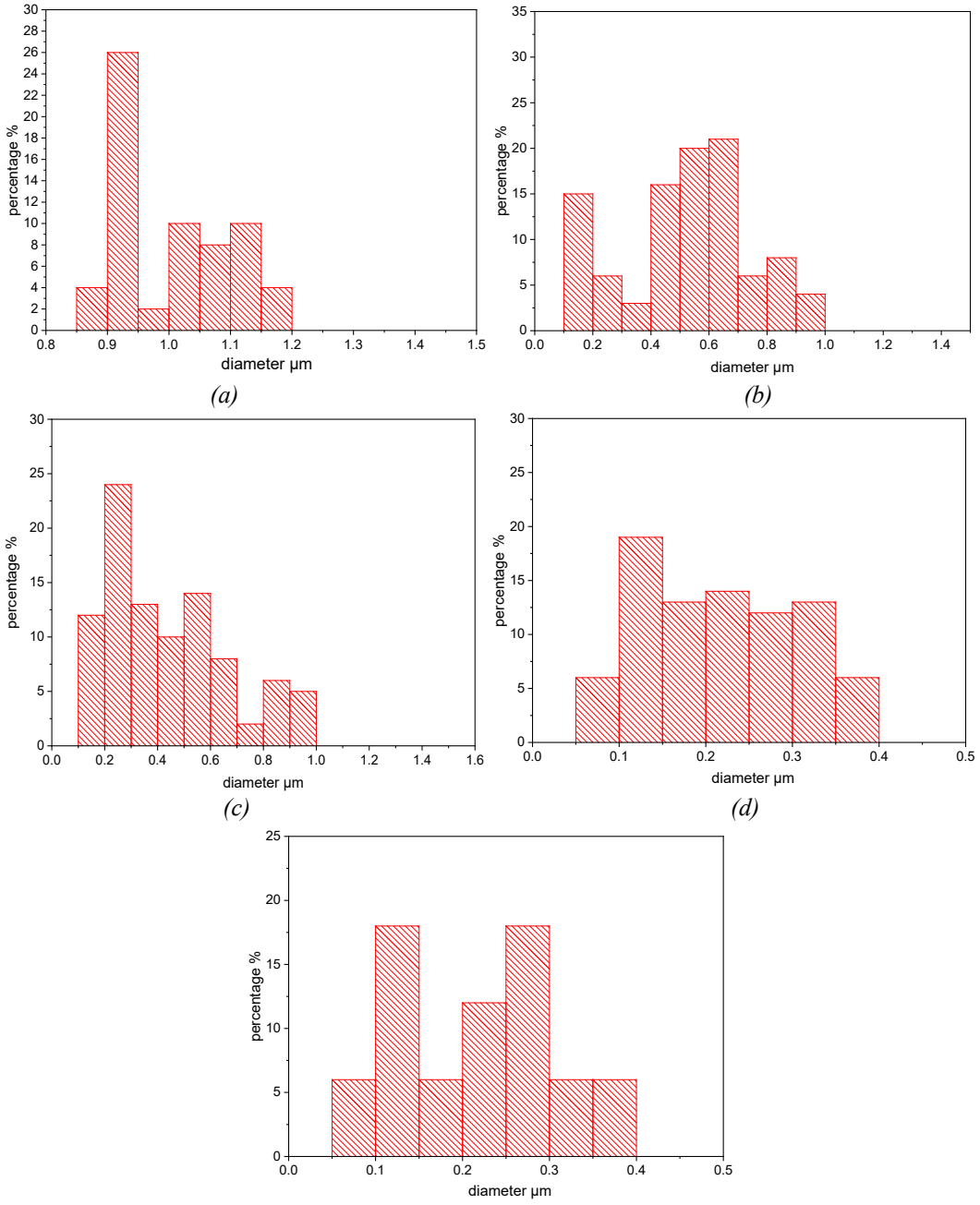

Fig. 8. Depicts the size histogram of AgNPs of (a) non-laser illuminated substrate and with different LPD (b)250 c)300, d)350 and e) 400) mW/cm^2.

In general, the spot region among the AgNPs was decreased and the best condition with minimum dimension of the hotspot vacancies ranging from (0.1-0.8) µm is found with 350 mW/cm^2.

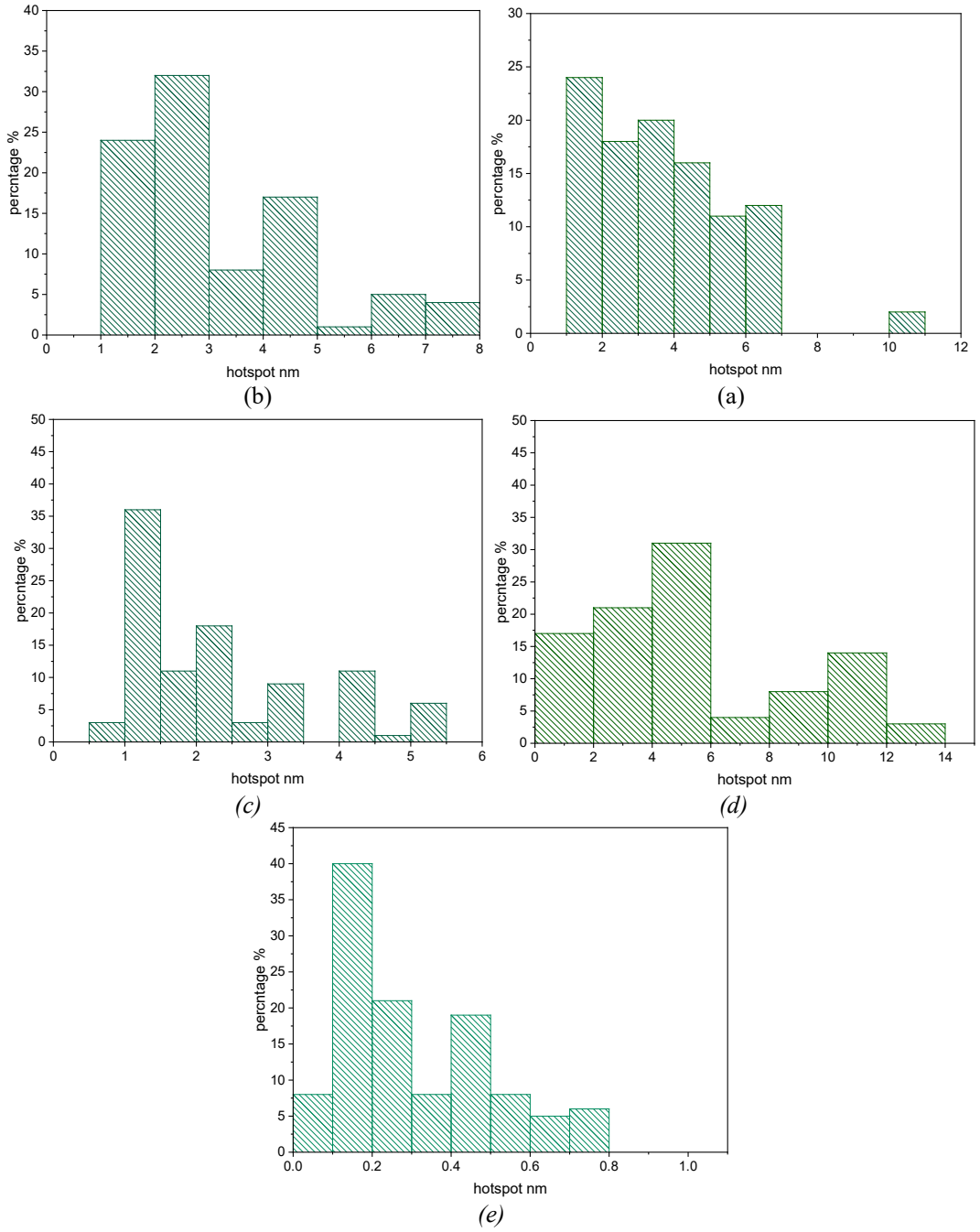

Fig. 9. Depicts the size histogram of hotspot vacancies within the Si nanocrystal line /AgNPs of (a) non-laser illuminated substrate and with different LPD (b)250 c)300, d)350 and e) 400)mW/cm^2.

The PL spectra of the Si substrates is shown in Fig 10 for Si crystalline with illumination 300, 350, and 400 mW/cm^2. The intensity of PL spectra are regularly depending on the density of Si nanocrystallites inside the formed layer. While the peak position of PL spectra depends on the quantum confinement process inside the nanocrystallites, the blue shifting of the peak position is due to the decreasing nanocrystal lite size under various conditions, the highest value of photoluminescence will grow due to the porosity. No PL emission was recorded under laser illumination of 250 and 300 mW/cm^2 due to the absence of silicon Nano crystallites, while specific emission were recorded under 350 and 400 mW/cm^2 due to the formation of porous like structure in Si substrate.

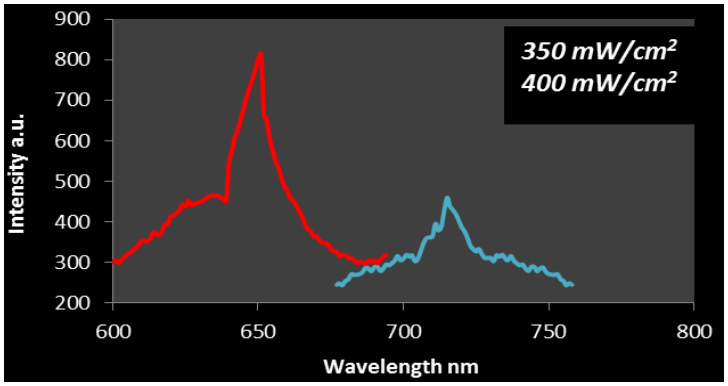

Fig. 10. Illustrates the PL spectra of Si Nano crystallites with illuminated at different power density.

Table 1 lists the PL wavelength, intensity of peak, energy gap, and average size silicon nano size.

Table 1. Illustrates the band gap energy, emission wavelength and Si Nano-size for different power density.

laser intensity	intensity (a.u.)	wavelength (nm)	Eg (psi) (eV)	L (A^0)
Non illuminated	/	/	/	/
250 mW/cm^2	/	/	/	/
300 mW/cm^2	/	/	/	/
350 mW/cm^2	**460**	**715**	**1.73**	**3.75**
400 mW/cm^2	**814**	**651**	**1.91**	**3.14**

For substrates with reduced silicon nano dimensions, the energy band gap was attained at 400 mW/cm^2 with an Eg value as high as 1.91 eV. Each crystallite is related with the increase in PL intensity. An rise in PL intensity, which represents the relation between nanocrystal size and structure. [14- 18]

Figure11, displays the XRD patterns of the generated Ag nanoparticles / Si nanocrystallites, which are created by integrating with and without laser illumination. These graphs showed that Si nanocrystallites, that have a 2θ diffraction angle of about 33.4°, are still in their crystalline phases along the 100 plane, while the XRD of Ag nanoparticles exhibits distinct Bragg's reflections.

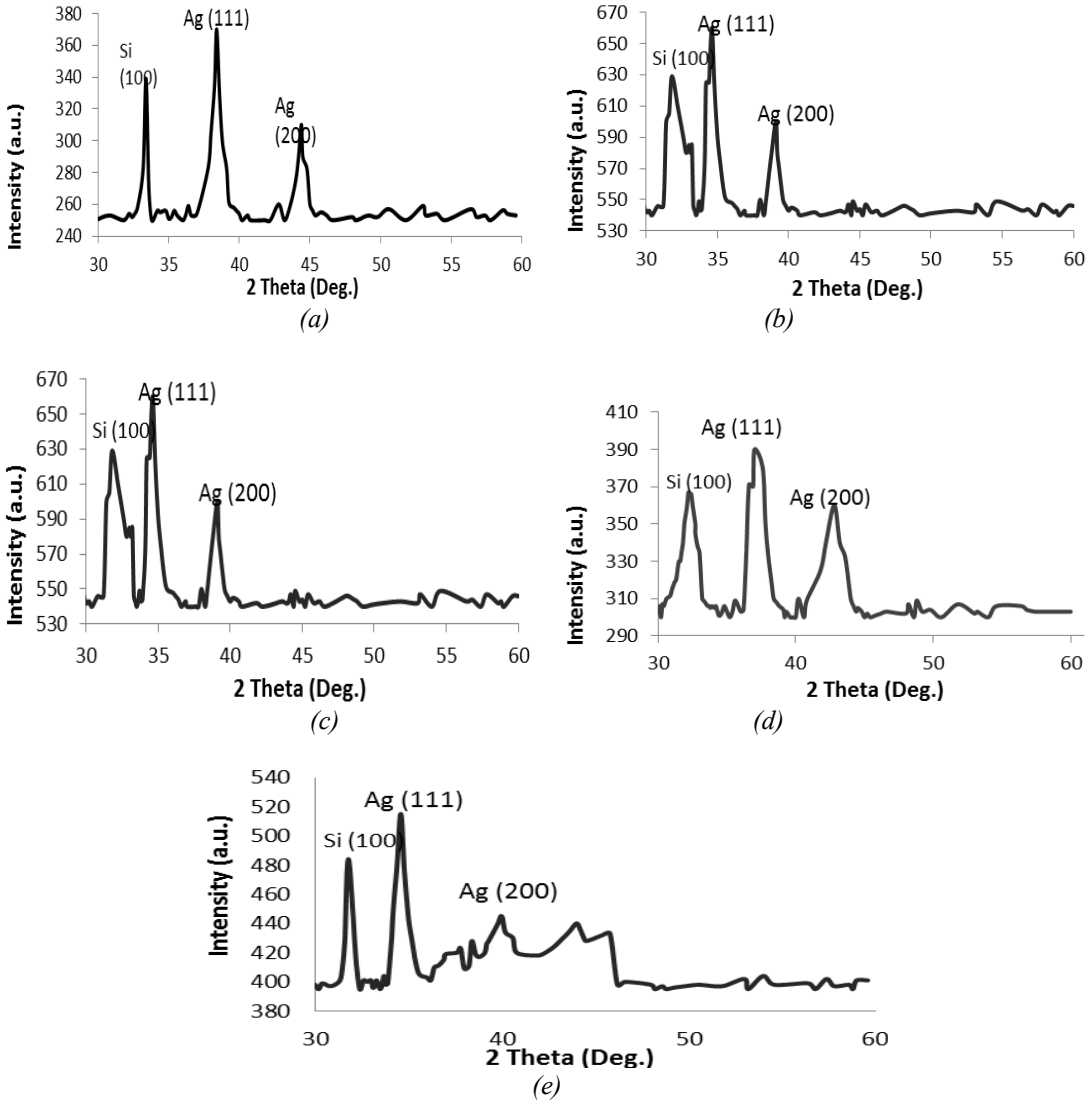

Fig. 11. Illustrates the XRD of Si nanocrystallites /Ag nanoparticles layer of laser illuminated substrates with different LPD. a) without illumination, b)250 mW/cm^2.c) 300 mW/cm^2 d) 350 mW/cm^2 e) 400)mW/cm^2.

By using Scherer's equation and the XRD peak widening, the grain sizes of the deposited silver nanoparticles were determined [18, 19]. The specific surface area (S.S.A.), which may be computed from equation(3), is a crucial parameter for characterization[20]:

$$S.S.D = 6000/\beta * \text{grain size} \quad (3)$$

where β is Ag density (10.49 g/cm^3) . Table 2 lists the amounts of Ag NPs grain sizes, (FWHM) and (S.S.A.) for plasmonics NPs with different illumination.

Table 2. The grain sizes, S.S.A. and FWHM values of Ag nanoparticles.

Power density (mW/cm^2)	peaks	FWHM (Deg)	Grain size (nm)	SSD m^2/g
Non illumination	111	1.361	6.1710	92.687
250	111	1.767	4.759	120.191
300	111	2.390	3.504	163.246
350	111	4.084	2.037	280.847
400	111	2.578	3.228	177.186

From this table, the biggest value of grain size is about 6.171 nm in the plane (111) for the substrate without illumination, while the lower value of grain size is in the plane (111) is around 2.037nm for the substrate with 350mW/cm^2 laser illumination. for the substrate with 350mW/cm^2 power density, a higher value of S.S.A for Ag NPs is achieved about 280.847m^2/g. whereas the lower value of about 92.687m^2/g is for the substrate without illumination. The Lessing rise of S.S.A and grain sizes of Ag NPs can be clarified rely on the Si nano crystallites aspects; mainly the surface roughness and the depth of base substrate.

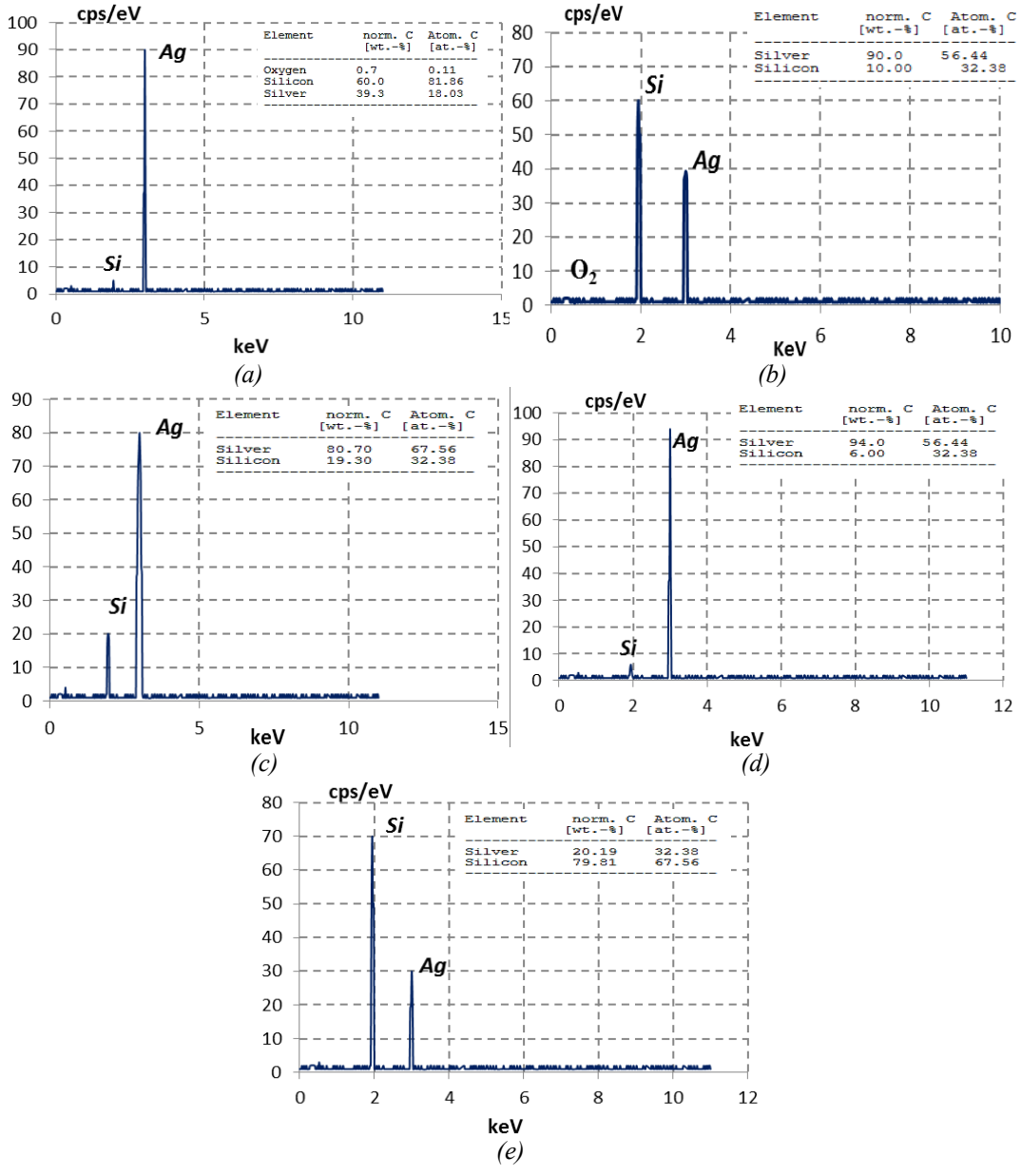

Fig. 12. EDS analysis of AgNPs/Psi hybrid structures of (a) non-laser illuminated substrate and with different LPD (b)250 c)300, d)350 and e) 400)mW/cm^2.

Figure (12a,b,c,d and e) shows the EDS spectra of monometallic AgNPs with various percentages deposited on the Psi layer as a function of LPD (250-400) mW/cm^2. The variance in the nucleation sites (dangling bond groups) on the Si surface lead to the variation in the amount of the deposited NPs. By raising the LPD, the amounts of specific NPs were raised. Additionally, at fixed LPD, the density of the deposited nanoparticles increased as the amount of electrons require for ion-reduction process to create the nanoparticles decreased. [20-26].

4. Conclusions

This work present a novel study which has been modified the nanoparticles by ion reduction process by using different laser irradiation intensity. The surface morphology of both Si nanocrystallites and AgNPs were modified according to the values of the laser intensities. The AgNPs were formed naturally with ion reduction process with small dimensions and non-homogenous morphologies. In comparison with the non-illumination case, the surface can be obtained the aggregation into cluster of layer for AgNPs, while when applied laser with different intensity the nano size and hot spot region will decreased with intensity in reverse relationship. No PL record for low laser intensity because the AgNPs will covered and absence the silicon nanocrystallites.

Using laser illumination during the ion reduction process, a simple, inexpensive, speedy, and well-controlled method for the production of plasmonic Ag nanoparticles on silicon nanocrystalites was carried out.

Acknowledgments

The authors would like to express their gratitude to the Department of Applied Sciences/University of Technology and Razi metallurgical research center, Iran, for using the SEM(MIRA3 TESCAN) and the EDS analyses.

References

[1] Liu K, Qu S, Zhang X, Wang Z, J Mater Sci 48:1755-1762, (2013); https://doi.org/10.1007/s10853-012-6936-7

[2] Weidemann S, Kockert M, Wallacher D, Ramsteiner M, Mogilatenko A, Rademann K et al (2015J Nanomater 16:171; https://doi.org/10.1155/2015/672305

[3] Huang Z, Fang H, Zhu J, Adv. Mater, vol.19, p.744-748, (2007); https://doi.org/10.1002/adma.200600892

[4] Choi WK, Liew TH, Dawood MK, Smith HI, Thompson CV, Hong MH, Nano Lett, vol. 8, p.3799-3802, 2008; https://doi.org/10.1021/nl802129f

[5] Chang S-W, Chuang VP, Boles ST, Ross CA, Thompson CV, Adv. Funct Mater,vol. 19, p. 2495-2500, 2009; https://doi.org/10.1002/adfm.200900181

[6] Hochbaum AI, Chen R, Delgado RD, Liang W, Garnett EC, Najarian M et al., Nature 451:163-167; https://doi.org/10.1038/nature06381

[7] R. B. Rashid, A.M. Alwan, M.S. Mohammed, Materials Chemistry and Physics, V. 293, 126898, 2023; https://doi.org/10.1016/j.matchemphys.2022.126898

[8] Wang F-Y, Yang Q-D, Xu G, Lei N-Y, Tsang YK, Wong N-B et al , Nanoscale 3:3269, 2011; https://doi.org/10.1039/c1nr10266d

[9] Peng F, Su Y, Ji X, Zhong Y, Wei X, He Y, (2014) Biomaterials 35: 5188-5195; https://doi.org/10.1016/j.biomaterials.2014.03.032

[10] Chartier C, Bastide S, Lévy-Clément C, (2008) Electrochim Acta 53:5509-5516; https://doi.org/10.1016/j.electacta.2008.03.009

[11] A. A. Khalaf, A. H. Attallah, A. B. Dheyab, and A. M. Alwan, Journal of Physics: Conference Series, V.1963, 012-015, 2021; https://doi.org/10.1088/1742-6596/1963/1/012015

[12] R. B. Rashid, A. B. Dheyab and A.M. Alwan, Optical and Quantum Electronics; https://doi.org/10.1007/s11082-021-03464-z

[13] Wang Z, Gong J, Ma J, Xu J., RSC Adv 2014:4(28):143-14; https://doi.org/10.1039/C4RA00160E

[14] Ruqaya, A.S and Mohammed, S.M., Applied nanoscience, 2018; https://doi.org/10.1007/s13204-018-0805-x

[16] LA Wali, KK Hasan, AM Alwan, Plasmonics 15 (4), 985-993, 2020; https://doi.org/10.1007/s11468-019-01096-4

[17] AM Alwan, RB Rashid, AB Dheyab, Iraqi Journal of Science (IJS) 59 (1A), 2018; https://doi.org/10.24996/ijs.2018.59.1A.8

[18] AA Jabbar, AM Alwan, MQ Zayer, Materials chemistry and physics ,122-359, 2020; https://doi.org/10.1016/j.matchemphys.2019.122359

[19] AM Alwan, Eng. & Tech. 25, 1143-1148, 2007.

[20] Detlef, M. S., J. Appl. Cryst 42, 1030-1034 (2009); https://doi.org/10.1107/S0021889809040126

[21] Duaa, A. H., Alwan, M. A., & Muslim, F. J., International Journal of nanoelectronics & material, 11, 461-472 (2018).

[22] Zhai, C., Li, Y., Peng, Y. & Xu T., Int. J. Agric. & Biol. Eng. 8, 113-120 (2015).

[23] Liu, Y., Zhang, Y., Wang, H., &Ye, B., Int J Agric & Biol Eng, 9(2), 179－185 (2016).

[24] Virga A, Rivolo P, Descrovi E, Chiolerio A, Digregorio G, Frascella F., (2012) J Raman Spectrosc 43:730-736; https://doi.org/10.1002/jrs.3086

[25] Devarajan S, Vimalan B, Sampath S, Colloid Interface Sci 278:126-113, (2004); https://doi.org/10.1016/j.jcis.2004.05.038

[26] Alwan,M. A., Dheyab, A.B. & Allaa, A.J., Engineering and Technology Journal vol.8, p. 811-815 2017; https://doi.org/10.30684/etj.35.8A.4

[27] A.M. Alwan, A.A. Yousif, L.A. Wali, Indian J. Pure Appl. Phys.vol. 55, p. 813-820, 2017.

[28] A.M. Alwan, A.A. Jabbar, A.J. Haider, Plasmonics, p. 1-12, 2017.

[29] Alwan M. Alwan, Amer B. Dheyab, Duaa A. Hashim, Layla A. Wali, Optik

[30] Alwan M. Alwan, Layla A. Wali, Khulood K. Hasan, Spectrochimica Acta Part A: Molecular and Biomolecular Spectroscopy, 206, p. 31-36, 2019; https://doi.org/10.1016/j.saa.2018.07.103

[31] Ismail, R.A., Khashan, K.S. & Alwan, M.A, Silicon 9, 321-326 (2017); https://doi.org/10.1007/s12633-016-9446-4

[32] Alwan, A.M., A.A. Jabbar, Modern applied science, 5(1), p. 106, 2011; https://doi.org/10.5539/mas.v5n1p106